International Journal of Automotive Technology, Vol. 6, No. 2, pp. 87−93 (2005)

1229−9138/2005/020−02

ANALYSIS OF THE SUITABLE INJECTION PRESSURE FOR DIESEL INJECTION WITH HIGH PRESSURE

D. Y. JEONG[1)*] and J. T. LEE[2)]

[1)]Department of Mechanical Engineering, Graduate School Sungkyunkwan University, Suwon, Gyeonggi 440-746, Korea

[2)]Department of Mechanical Engineering, Sungkyunkwan University, Suwon, Gyeonggi 440-746, Korea

(Received 30 August 2003; Revised 27 February 2004)

ABSTRACT–Spray patterns were visualized using the shadowgraph method, and the droplet size and velocity were measured using PDPA for high-pressure injections up to 2,600 bars. The spray pattern and spray characteristics, such as penetration, spray width, spray angle, droplet size, injection duration, and droplet velocity, were investigated to determine the suitable injection pressure. Spray penetration, width, angle, and velocity increased continuously up to 2,600 bars with the injection pressure in a high-pressure region. The rate of improvement of the above spray characteristics, however, declined rapidly, when the injection pressure reached 2,000 bars. The injection duration and droplet size generally decreased with the increase in the injection pressure, while the rate of improvement decreased abruptly after 2,000 bars. Consequently, the improvement rate of the spray characteristics became blunt at over 2,000 bars. This means that the suitable injection pressure is around 2,000 bars.

KEY WORDS : Ultra high pressure injection, SMD (Sauter mean diameter), Spray visualization, Spray characteristic, Suitable injection pressure, PDPA (Phase doppler particle analyzer)

1. INTRODUCTION

High-pressure fuel injection is an excellent method of promoting atomization of fuel. Atomization by high-pressure injection can reduce both particulate and fuel consumption, and can increase engine power. The temperature of combustion gas can be decreased by retarding the injection timing. This results in the reduction of NOx. To investigate the utility of high-pressure injection, Kato *et al.* (1989), Keiya *et al.* (1997), Pierpont *et al.* (1995), and Stump *et al.* (1989) clarified that spray characteristics were improved continuously under 2,000 bars.

The spray and combustion characteristics will be improved to some degree when the injection pressure is increased to an ultra-high pressure. The improvement rate of the spray and the combustion characteristics, however, are expected to decrease with the increase of the injection pressure. A suitable injection pressure, which makes the improvement rate of the spray characteristics blunt, is thus expected. Furthermore, if the injection pressure becomes ultra-high, the spray from the nozzle converts to a critical state, indicating that there is a limit to the improvement of spray characteristics, or that the spray characteristics may get worse. A higher-pressure injection system is more costly due to the difficulty in control its ability and durability. Therefore, it is necessary to find a suitable injection pressure when the injection pressure becomes ultra-high. Because of the difficulty in inventing an ultra-high-pressure injection equipment that is necessary to analyze pressure, studies on high-pressure injection under 2,000 bars have been conducted up to now.

In this paper, a suitable injection pressure is investigated from a free-spray pattern injected into the air. An ultra-high-pressure injection equipment that is able to reach over 4,000 bars has been developed to investigate a suitable injection pressure. Spray was visualized, and droplet size and injection duration were measured up to 2,600 bars, to investigate a suitable injection pressure from the viewpoint of the improvement rate of the spray characteristics.

2. TESTING DEVICE AND METHOD

2.1. Testing Device

2.1.1. Ultra-high-pressure injection equipment (UHPIE)
The UHPIE must be able to maintain ultra-high pressure. The injection pressure and timing should be controllable, and the injection pattern and curve should be similar to

**Corresponding author.* e-mail: dyjeong@skku.edu

those of an actual engine. Considering the above concepts, a single-shot UHPIE was developed and is shown in Figure 1. The UHPIE consists of a 1st-stage compression component, a 2nd-stage compression component, a returning component, and an injector. A detailed description of the UHPIE follows.

1st-Stage Compression Component: This equipment, which pressurizes the fuel supplied to the plunger, consists of a fuel tank and a pressurizing cylinder that pressurizes the cylinder without bubbles. A 200-bar booster cylinder was used for the 1st fuel pressurization. The hydraulic pump was used to control the 1st pressurization of the fuel.

2nd-Stage Compression Component: This equipment, which re-pressurizes the fuel using the 1st-stage compression component, consists of an N_2 gas bomb, a high-pressure accumulator, including operating oil, a stopper, and a plunger pump. Inert N_2 gas was used to pressurize the operating oil and to prevent self-ignition by mixing the operating oil with air. The plunger velocity is changed with the pressure control of the operating oil, and its pressure is controlled by the regulator. The high-pressure accumulator has a 30-liter container that is big enough to prevent a rapid pressure drop when a large quantity of operating oil is sent to the plunger-driving cylinder. The diameter of the plunger-driving cylinder is 140 mm. When the working fluid pressure is 80 bars, the maximum design compression pressure of fuel that can be pressurized by the plunger-driving cylinder is about 12,000 bars.

An actual and repeatable injection pressure, with the use of this equipment, is around 4,200 bars. The distance between the end of the cylinder rod and the tappet of the plunger pump is maintained to transfer enough kinetic energy to the plunger pump. The plunger is used in a commercial-type PE-P, and its diameter is 12 mm and its effective stroke, 5 mm.

The injection quantity is controlled using the control rack position changer. The plunger barrel is held by a plunger holder, and the delivery valve is installed at the upper side of the holder. The inlet port and the air drain holes are installed to deliver the pressurized fuel to the plunger barrel, and to remove the bubble installed at the side of the holder, respectively.

Returning Component: This equipment consists of the returning hydraulic cylinder, the plunger-driving cylinder, and the hydraulic pump. The return cylinder is installed at the base of the plunger-driving cylinder, and is operated by the hydraulic oil pump. The return cylinder elevates the stopper up to the end of the rod of the plunger-driving cylinder. The stopper goes up to the end of the rod, and locks it. The returning cylinder pulls down the rod to restore it to its initial position.

Injector: The multi-hole injector (DLL-s type), using a direct-injecting diesel engine, was modified. The modified injector consists of a nozzle holder, a nozzle, a pressure spring, a needle lift sensor, and a screw to control the spring tension. The opening pressure of the nozzle is adjusted by controlling the tension of the pressure spring.

To measure the needle lift, a pressure pin through the center of the pressure control screw transfers the movement of a needle, and is adjacent to the gap-sensor-mounted top of the injector. The hole diameter is 0.23

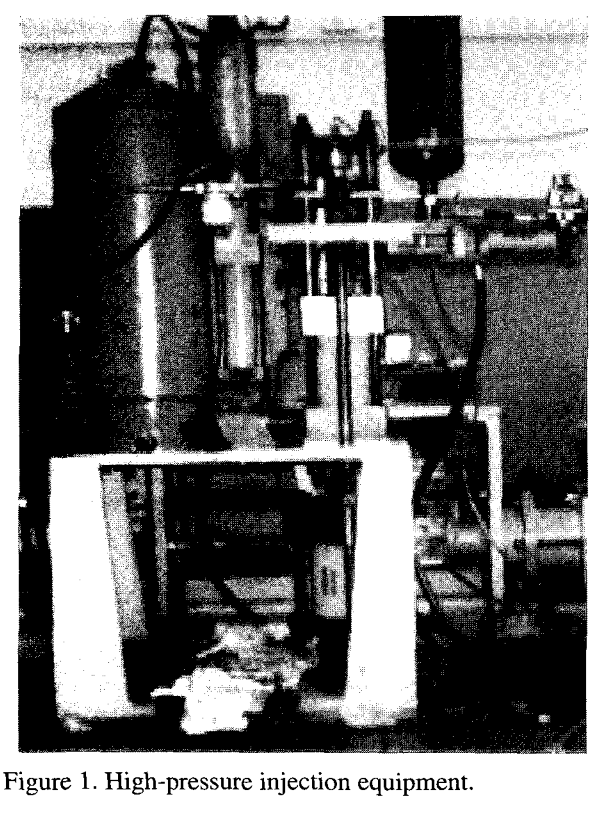

Figure 1. High-pressure injection equipment.

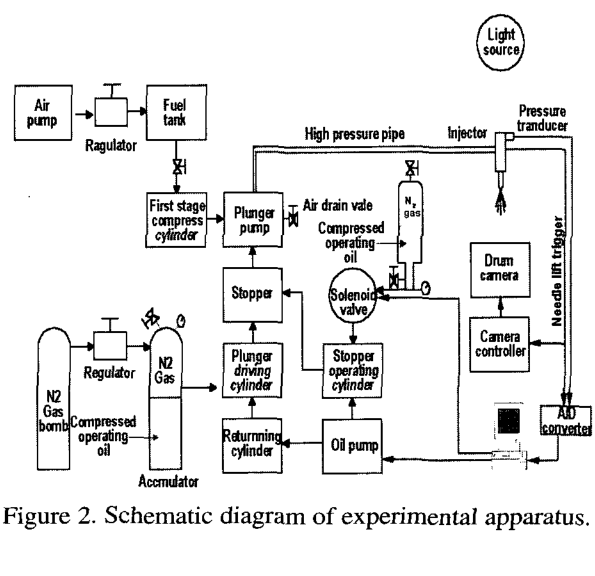

Figure 2. Schematic diagram of experimental apparatus.

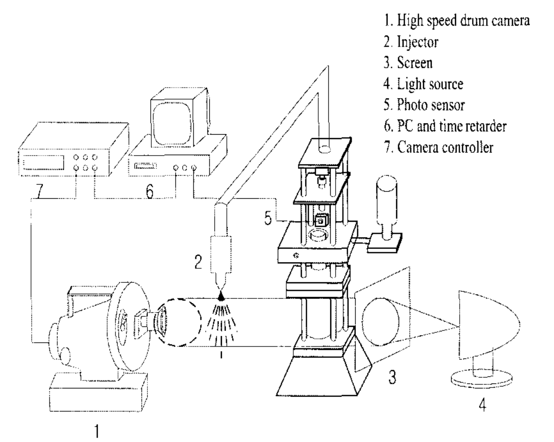

Figure 3. Visualization system for a high pressure spray.

mm, the injection angle is 150°, and the needle lift is 0.3 mm. It has five holes.

2.1.2. Analysis system of spray characteristics in high pressure

The testing device for measuring the spray characteristics in high pressure is shown in Figure 2. The testing device consists of a UHPIE, a visualization system, a Phase Doppler Particle Analyzer (PDPA), and data acquisition and control systems. A high-speed camera (Cordin 350), capable of 35,000 frame/sec is used to measure spray characteristics, such as spray tip penetration, spray width, and spray angle. The halogen lamps (650 W × 2) were used as a light source. Semi-transparent paper is installed between the camera and the light to prevent direct exposure to light. The schematic diagram for spray visualization is shown in Figure 3. The droplet size was measured using a PDPA, which consisted of a fiber driver, a transmitter, a receiver, a signal analyzer, and a PC.

A Piezo-type pressure transducer, which is able to measure up to 10,000 bars, was mounted to measure the injection pressure in the fuel supply line before the injector. The needle lift length was measured using the capacity-type gap sensor (VE-231), which has a measuring range of 0–2 mm.

Data on the fuel injection pressure and the needle lift signal were converted using the A/D converter, and were analyzed in the PC.

2.2. Testing Method

The purpose of this study is to analyze free-spray characteristics on ambient conditions. One of the experimental conditions is injection pressure. Injection pressure was changed step by step, from 1,000 bars to 2,600 bars. The opening pressure of the injector was fixed at 500 bars. The spray was visualized using the shadowgraph method. The droplet size was measured at 60 mm from the nozzle tip.

3. SPRAY CHARACTERISTICS IN A HIGH PRESSURE REGION

3.1. Spray Behavior

Figure 4 shows the visualized photograph of the spray behavior up to 2,600 bars, with the lapse of time.

The fuel sprays show that the shape of the spray is straight, that its edge is sharp at the early stage of injection, and that it was smooth for all injections. The spray edges became dull, and the sprays became shaky, with the lapse of time, and these tendencies increase with higher injection pressure conditions. The shaking of the sprays was expected to result from the increase of the mutual reaction between air and the spray, with the progress of the spray from the nozzle tip.

As the injection pressure increased, the above aspects became greater because the sprays were shaky, widely due to the higher injection pressure.

The amount of the droplets, which were spread from the surface of the spray to the axis and radius directions, increased with the increase of the injection pressure, and the same tendency was repeated in high-pressure injections. It was shown, however, that the droplets that spread to the axis and radius directions did not increase remarkably over 2,000 bars.

The data were analyzed quantitatively with visualized photographs, as follows.

3.2. Spray Tip Penetration and Droplet Velocity

Figure 5 shows the spray tip penetration with the time lapse at the high-pressure injection.

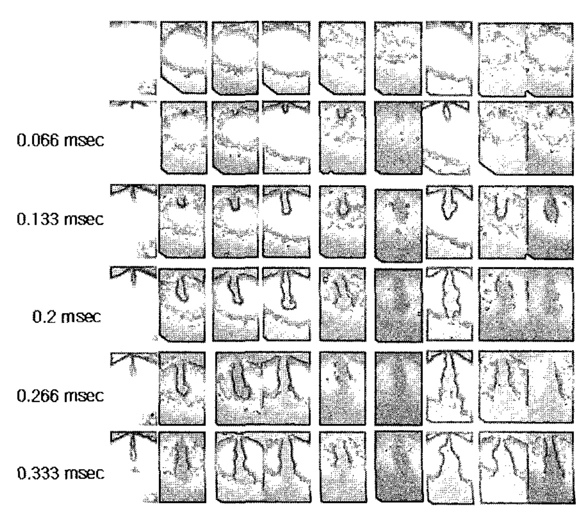

Figure 4. Spray behavior versus injection pressure with the lapse of time.

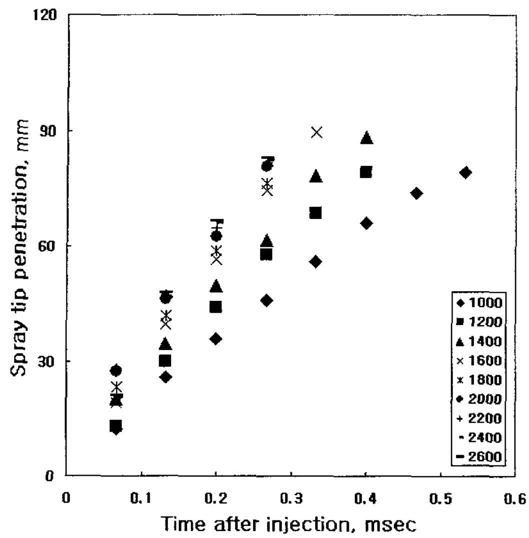

Figure 5. Spray tip penetration versus injection pressure with the lapse of time.

Spray tip penetration was defined from the nozzle tip to the end of the spray for the vertical direction. It increased continuously with the time lapse, and also increased with the increase of the injection pressure. The rate of increase, however, became blunt with the increase of the injection pressure, and decreased remarkably over the 2,000-bar injection pressure.

When the injection pressure reached 1,800 bars, it increased by 62.6% in comparison with the 1,000 bars at the time of 0.266 ms after injection.

When the injection pressure became higher (up to 2,000 bars), penetration increased by 15% compared with the pressure of 1,800 bars. When the injection pressure was set at 2,600 bars, the increase in the rate of penetration was only 4.2%.

The spraying energy increased due to the increase of the spray velocity, but was reduced with the decrease of the droplet size, as will be mentioned in Section 3.4, with the increase of the injection pressure. The above velocity and size effects on spray tip penetration offset each other. The spray energy was similar at over 2,000 bars. Therefore, it is thought that the increasing rate of penetration became blunt when the injection pressure was over 2,000 bars, according to the above results.

In other words, as shown in Figure 6, the maximum velocity increased with the increase of the injection pressure, but the spray tip penetration increased only slightly over a 2,000-bar injection pressure due to the decrease in kinetic energy through the atomization of droplets.

3.3. Spray Width and Spray Angle

Figure 7 shows the spray width with the time lapse of

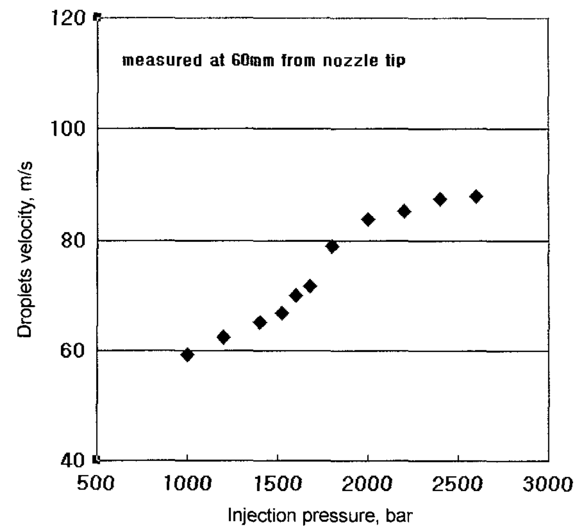

Figure 6. Droplets velocity versus injection pressure.

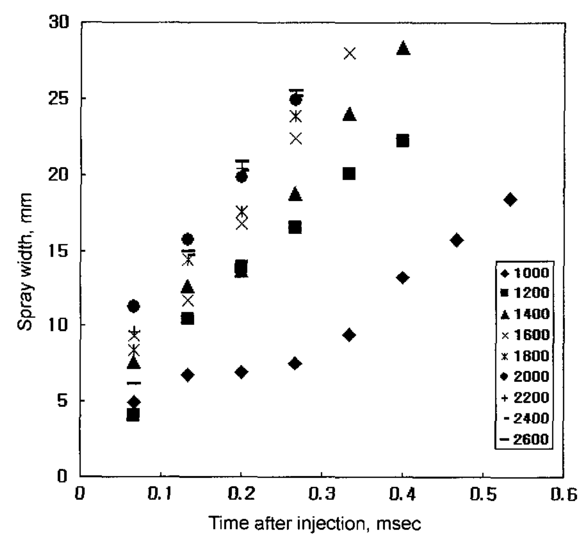

Figure 7. Spray width versus injection pressure with the lapse of time.

each injection pressure. The spray width is defined with the distance, which is widest from the left side to the right side of the spray. At the early stage of the injection, the spray width increased with an increase of the injection pressure up to 2,000 bars, but when the injection pressure became much higher, the spray width decreased rather. The spray width, however, increased with the time lapse in case of high pressure. The tendency of the spray width to increase is similar to that of the injection pressure after 0.2 ms. The mutual reaction between air and the fuel is increased by increasing the droplet velocity and by increasing the injection pressure, as shown in Figure 6. Atomized droplets are spread far away to the radius direction. Therefore, spray width is increased with an

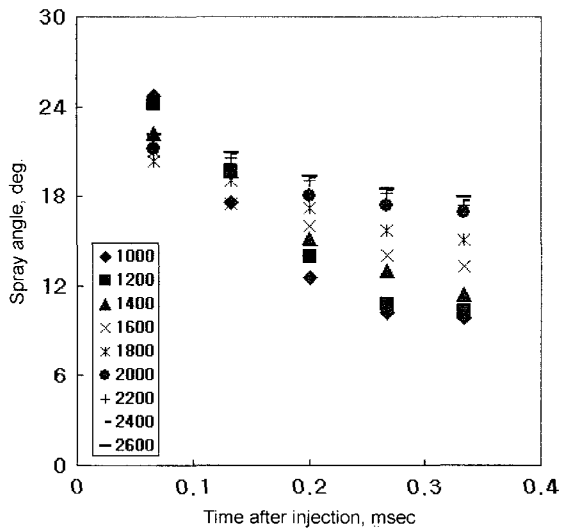

Figure 8. Spray angle versus injection pressure with the lapse of time.

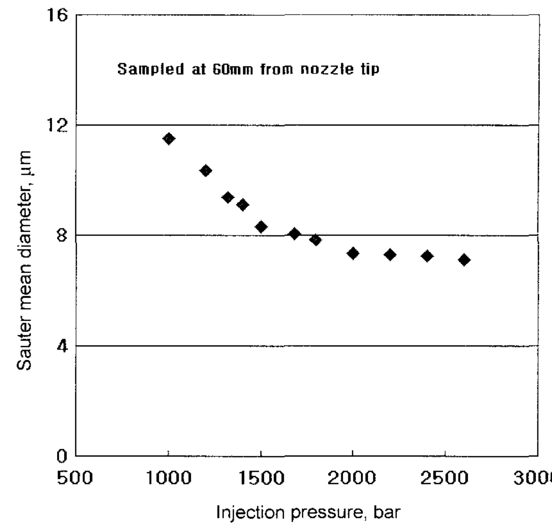

Figure 9. Droplets size versus injection pressure.

increase of the injection pressure. The rate of increase of the spray width, however, becomes blunt, and it is about 8% when the injection pressure reaches over 2,000 bars.

For example, if the injection pressure is set at 2,000 bars from 1,000 bars, the ratio of increase of the spray width is remarkable about 232%. At 2,600 bars, it increases by about 240%. The rate of increase of the spray width up to 2,600 bars is just 2.4%, however, compared with 2,000 bars.

The spray angle results from spray tip penetration and spray width are shown in Figure 8. The spray angles decreased with the time lapse for each injection pressure, and then converged after a while.

In case the injection pressure is within a low range, the spray angle is bigger at the early stage of the injection. The spray angles increase, however, with increasing injection pressure, with the time lapse. The changes in the spray angle between the beginning and the end of the injection are large in case of a low-pressure range. As the injection pressure becomes higher, however, those results become smaller. The spray angle increases due to the increase of the spray width with the increase of the injection pressure, and its rate of increase is shown to decrease remarkably over 2,000 bars. The spray angle was increased by approximately 7° and 8° when the injection pressure increased from 1,000 bars to 2,000 bars and 2,600 bars.

3.4. Droplet Size (SMD)

Figure 9 shows the droplet size for the injection pressure as SMD. The droplet size decreased continuously with the increase of the injection pressure. Its rate of decrease went down with the increase of the injection pressure, however, and it became almost the same size, when the injection pressure was over 2,000 bars. The droplet size decreased, and the rate of decrease became blunt, with the mutual reaction between air and the droplets due to the continuous increase in the droplet velocity with the increase of the injection pressure.

When the injection pressure increased from 1,000 bars to 2,000 bars, the droplet size decreased remarkably from approximately 11.5 μm to approximately 7.34 μm, but when it was over 2,000 bars, the droplet size became approximately 7 μm.

This means that the degree of vaporization of fuel by the surface that is contacted between the air and the fuel, and the improvement of the combustion characteristics, are limited.

3.5. Injection Duration

Figure 10 shows the injection duration for high-pressure injection. The injection duration was measured by needle lift. It was defined with a needle-lifting duration because the injection duration is accordant with the needle valve opening time. The injection duration generally decreased with the increase of the flow of fuel due to the increase of the injection energy with the increase of the injection pressure. The injection duration decreased linearly until 2,000 bars, and decreased moderately over 2,000 bars.

Massanori (1994) and Kato (1989) clarified that the injection duration also decreases with an increase of the injection pressure. CO and smoke were decreased with the increase of the injection pressure. It is thought that this is caused by the decrease of the injection duration and the enhancement of atomization and fuel distribution with the increase of the injection pressure. As previously mentioned, although the injection pressure becomes

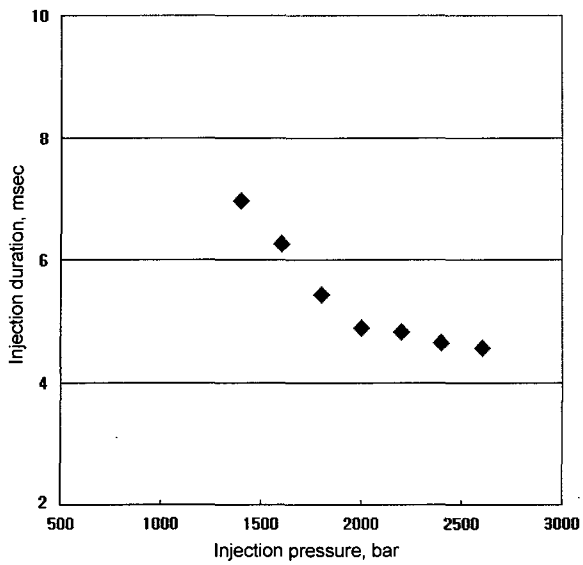

Figure 10. Injection duration versus injection pressure.

higher, the injection duration, droplet size, and penetration are not much different over a 2,000-bar injection pressure.

This indirectly shows that the effect of decreasing exhaust gas, such as CO or smoke, has not developed much over a 2,000-bar injection pressure.

3.6. A Suitable Injection Pressure

Figure 11 shows the enhancement ratio of spray characteristics such as spray tip penetration, spray width, droplet size, and injection duration. As shown in this figure, the above characteristics generally increase with the increase of the injection pressure. It is also shown that the improvement rate of spray characteristics becomes blunt over a 2,000-bar injection pressure. When the injection pressure increased from 2,000 bars to 2,600 bars, the spray tip penetration and spray angle are enhanced by 4.2% and 1°, respectively. The droplet size is slightly enhanced by around 2.1%, and the injection duration is decreased by 4.2%.

As mentioned above, it is known that penetration, atomization, distribution of fuel, and injection duration are not improved remarkably in high-pressure regions over 2,000 bars.

This means that the suitable injection pressure is around 2,000 bars, from the viewpoint of the improvement rate of spray characteristics. A spray injected into an engine is an impinging spray against the piston head and the cylinder wall. Combustion, therefore, depends on this phenomenon.

A systematic analysis of the impinging spray and combustion characteristics in a high-pressure range is necessary to determine the most suitable injection pressure.

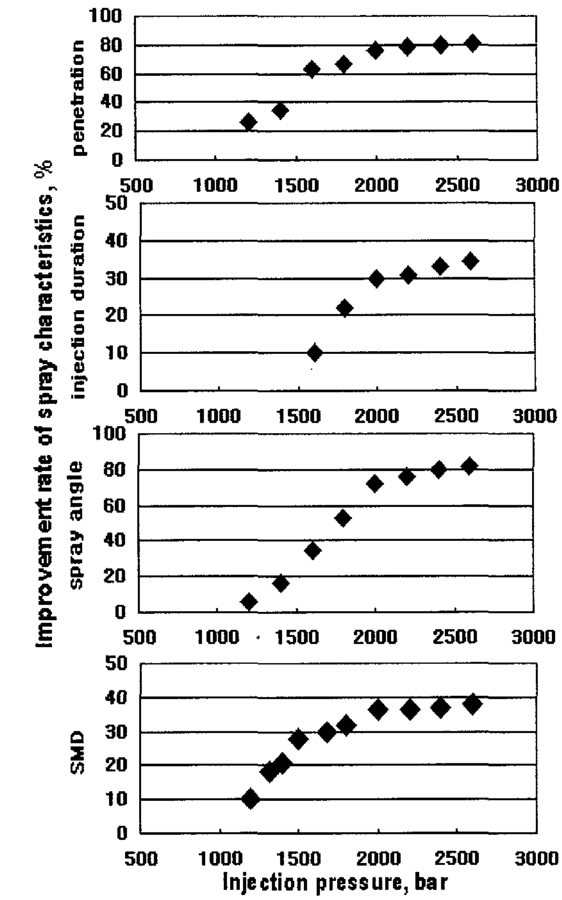

Figure 11. Spray characteristicses versus injection pressure.

4. CONCLUSIONS

From the above analysis of spray characteristics for different injection pressures in an ultra-high-pressure range, the following conclusions are arrived at : From the analysis of spray characteristics for different injection pressures within an ultra-high-pressure range, the conclusions are as follows:

An ultra-high pressure of over 4,000 bars is achieved by the developed UHPIE (Ultra-high-pressure injection equipment), and a foundation is established for the analysis of spray characteristics in ultra-high-pressure regions.

Spray spreading toward the axis and the radius direction increases with an increase of the injection pressure, but spray behavior patterns are similar at an injection pressure of over 2,000 bars.

Spray tip penetration, spray width, and spray angle improve continuously with an increase in the injection pressure to a high pressure of up to 2,000 bars, but the improvement rate remarkably slows down at over 2,000 bars.

The droplet velocity increases continuously at up to 2,000 bars, but the improvement rate decreases conspicuously at an injection pressure of over 2,000 bars.

Droplet sizes decrease generally with an increase in the injection pressure, but the improvement is not significant at over 2,000 bars, and the droplet size becomes about 7 μm.

From the above results, it can be concluded that the suitable injection pressure is around 2,000 bars, based on the viewpoint of the improvement rate of free-spray characteristics. This result comes from the analysis of free spray characteristics. Impinging spray characteristics and combustion characteristics will be required at a high pressure later on.

ACKNOWLEDGEMENT–This work was supported by Grant No. R01-2001-000-00386-000 (2003) from the Korea Science and Engineering Foundation and the BK21 project of the Ministry of Education.

REFERENCES

Jeong, D. Y., Lim, H. S. and Lee, J. T. (2002). A study of the characteristics of atomization in an ultra-high-pressure injection region. *Fall Conference Proc. Korean Society of Automotive Engineers*, 240–245.

Kato, T., Tsujimura, K., Shintani, M., Minami, T. and Yamaguchi, I. (1989). Spray characteristics and combustion improvement of a D. I. diesel engine with high-pressure fuel injection. *SAE Paper No.* 890265.

Keiya, N., Hiroaki, O., Masataka, A. and Hiroyuki, H. (1997). Characterization of diesel fuel spray by ultra-high-pressure injection. *J. Japan Society of Mechanical Engineering* **63, 605,** 344–349.

Masanori, K., Yoshinaka, T., Kinji, T. and Shigeru, S. (1994). Diesel combustion improvement and emission reduction using a VCO nozzle with high-pressure fuel injection. *J. Japan Society of Mechanical Engineering* **25, 1,** 45–50.

Pierpont, D. A. and Reitz, R. D. (1995). Effects of injection pressure and nozzle geometry on D. I. emission and performance. *SAE Paper No.* 950604.

Shundoh, S., Kakegawa, T. and Tsujimura, K. (1991). Effect of injection parameters and swirl on diesel combustion with high-pressure fuel injection. *SAE Paper No.* 910489.

Stump, G., Polach, W., Muller, N. and Warga, J. (1989). Fuel injection equipment for heavy-duty diesel engines for U.S. 1991/1994 emission limits. *SAE Paper No.* 890851.